BRAZE PROCESS OPTIMIZATION INVOLVING CONVENTIONAL METAL/CERAMIC BRAZING WITH 50AU-50CU ALLOY *

L. A. Malizia, K. Meredith, D. Appel, S. L. Monroe, S. N. Burchett and J. J. Stephens

Abstract

Numerous process variables can influence the robustness of conventional metal/ceramic brazing processes. Experience with brazing of hermetic vacuum components has identified the following parameters as influencing the outcome of hydrogen furnace brazed Kovar™ to metallized alumina braze joints: (a) Mo-Mn metallization thickness, sinter fire temperature and porosity (b) Ni plate purity, thickness, and sinter firing conditions (c) peak process temperature, time above liquidus and (d) braze alloy washer thickness. ASTM F19 tensile buttons are being used to investigate the above parameters. The F19 geometry permits determination of both joint hermeticity and tensile strength.

This presentation will focus on important lessons learned from the tensile button study: (A) the position of the Kovar™ interlayer can influence the joint tensile strength achieved - namely, off-center interlayers can lead to residual stress development in the ceramic and degrade tensile strength values. Finite element analysis has been used to demonstrate the expected magnitude in strength degradation as a function of misalignment. (B) Time above liquidus (TAL) and peak temperature can influence the strength and alloying level of the resulting braze joint. Excessive TAL or peak temperatures can lead to overbraze conditions where all of the Ni plate is dissolved. (C) Metallize sinter fire processes can influence the morphology and strength obtained from the braze joints.

Keywords: metal/ceramic brazing, process characterization, tensile buttons, Mo-Mn metallize, Ni plating.

INTRODUCTION

Despite the relative maturity of hermetic brazing with Mo-Mn metallized and Ni-plated alumina ceramic to controlled expansion alloys such as Kovar™ (Ref. 1), numerous parameters can influence the robustness of the brazing process. In order to conceptualize this particular brazing process, it is necessary to differentiate design factors, which can influence the robustness of a metal/ceramic braze joint, from the process variables that are used to obtain a completed braze joint. Due to the mismatch in thermal expansion between Kovar™ alloy and metallized alumina ceramic at temperatures >450°C (Ref. 2), there are a number of undesirable metal/ceramic braze joint geometries (Ref. 3). Metal/ceramic braze joint geometries, such as the "tortuous path" joint, do not permit accommodation of residual stresses across the joint by means of braze alloy stress relaxation. The absence of braze alloy stress relaxation in such joints occurs because triaxial stress states exist in the

---

* The authors are Members of the Technical Staff at Sandia National Laboratories, Albuquerque, NM 87185-0367. This work was supported by the US Dept. of Energy under Contract DE-AC04-94AL85000. Sandia is a multiprogram laboratory operated by Sandia Corporation, a Lockheed Martin Company, for the US Department of Energy.

DISCLAIMER

brazement that cannot be mitigated by creep deformation. Conversely, the most desirable metal/ ceramic braze joint geometries, which minimize residual stresses in the ceramic, are those where the brazement is loaded in shear (Refs. 3-4).

There are a number of process and material variables can influence the success of a metal/ceramic brazing process. The following items are the major material/process variables in the temporal sequence used for alumina ceramic brazing:

(A) Alumina Preparation: Brazing to bare alumina requires a braze alloy with the ability to form a metallurgical bond to alumina. However, only active braze alloys (i.e. braze alloys that contain active elements – Ti, Zr or V), have this ability. Most production braze processes do not employ these alloys. Therefore, there is a need to place a wettable material on the alumina ceramic surface. Placing a thin Mo-Mn metallization layer on the alumina creates the wettable surface. The metallize thickness, sinter fire temperature, as well as type of 94% alumina ceramic are important to the strength/bonding aspects of this metallized layer.

(B) Nickel Plating: A freshly metallized surface can be wet by conventional braze alloys. However, once the metallize is exposed to atmosphere for longer than a day, conventional brazing is marginal. Due to various inspection and other manufacturing restrictions, brazing within 24 hours of metallized sinter firing is impractical. Therefore, nickel plating of the metallized surface is used in order to produced and preserve a brazeable surface on the Mo-Mn metallize. This Ni plating is applied by electroplating and sinter fired (e.g., in a wet hydrogen atmosphere) at a much lower temperature than the metallized layer. The control of plating thickness and avoidance of blistering are key for hermetic braze joints.

(C) Braze Volume: Another important variable is the thickness and size of the braze preform (wire, washer, disk) used. The size of the preform directly influences the amount of braze volume present - with higher volumes generally causing increases in residual stresses in the ceramic within the completed joint. This braze volume effect is cause by the fact that the braze alloy has a thermal expansion coefficient considerably higher than that of Kovar™ alloy or alumina ceramic.

(D) Fixtures: In brazing ceramic to metal parts, fixturing is needed to ensure that the resultant brazed assembly meets the dimensional requirements. Metal marks on ceramic surfaces are usually unacceptable, so fixtures are generally made of alumina if they touch a ceramic part. The remainder of the fixture can either be alumina or metal. Another factor that is influenced by the fixture is the amount of weight placed on the joint. A minimum amount of weight is needed to ensure that the parts will remain in contact, but too much weight might cause expulsion of braze material from the joint onto surfaces where braze material is unacceptable.

(E) Temperature Profile: Potentially, the most important factor in the development of a successful brazement in the temperature profile that the joint experiences. The actual brazing parameters such as furnace ramp rate(s) (both heating and cooling), stabilization hold time, time above liquidus temperature (TAL) and peak temperature have a critical effect on the successful outcome. In general, with conventional braze alloys it is considered prudent to minimize the TAL during brazing. Minimization of TAL reduces the amount of base metal and/or Ni plate erosion and subsequent alloying of the braze joint (Ref. 5). In the case of brazed subassemblies which contain a single braze joint, minimization may be possible. However, in many situations with complicated part geometries, large fixture mass and multiple braze joints, one is often forced to modify the braze process to accommodate the most difficult braze joint. Finally, braze furnace hot zone uniformity, and control thermocouple locations provide another host of considerations; the reader interested in these specific issues should refer to a companion paper (Ref. 6) included in this volume.

The present study was motivated by the need to obtain detailed process characterization information on the conventional brazing of metallized alumina ceramic to Kovar™ (nominal composition: 54wt.%Fe-29Ni-17Co) parts using the 50wt.%Au-50Cu braze alloy. This particular braze alloy is

significant to component assembly production flow since it is used as a higher level step braze process. For example, step brazing process parts that have been brazed into "first level" assemblies using Oxygen Free Electronic Grade (OFE) copper are subsequently brazed using the 50Au-50Cu alloy. Consequently, those higher level assemblies that are scrapped following the 50Au-50Cu alloy braze process have a significant amount of value added from the production process into their overall cost. Due to the high cost and lack of availability of actual piece parts for higher level studies, process characterization can be conducted using the ASTM F19 tensile button design (Ref. 7). The F19 geometry permits determination of both joint hermeticity and tensile strength. Throughout the study discussed in this paper, we use a 0.010-inch thick Kovar™ interlayer with ID and OD dimensions identical to the ASTM F19 tensile button design.

In regards to any process characterization study, the critical issue becomes "how many related processes are to be included in the Design of Experiments?" As described earlier in this introduction, there are a number of related process variables that could be pursued. However, for the purposes of setting an extensive braze process characterization study (aptly named "Large Tensile Button Study" (LTBS), and discussed later in this paper), it was decided that a limited study (the "Small Tensile Button Study" (STBS)) would first be run. The purpose of the STBS was to examine the effect of metallization sinter firing on the strength and hermeticity of the tensile buttons brazed with the 50Au-50Cu alloy. This more limited study also provided an opportunity to evaluate the tensile button brazing fixture, and to assess whether any changes were needed prior to running the LTBS.

DESCRIPTION OF THE SMALL TENSILE BUTTON STUDY

A total of twenty-four F19 tensile buttons pairs were prepared for this study. All tensile buttons were fabricated from Diamonite grade P-3142-1 alumina ceramic, supplied by Specialty Ceramics Division of Ferro Corporation. This nominal 94% alumina ceramic is composed primarily of α-alumina with SiO_2, Al_2O_3, CaO and MgO serving as the major constituents of the glass (grain boundary) phase. All tensile buttons were screen printed with WESGO 538S Mo-Mn metallize ink. Twelve pairs of buttons were subjected to a "normal", 45 minute metallization sinter fire at 1495°C in wet hydrogen, and the second set of twelve pairs were processed using an "extended" sinter fire consisting of 120 minutes at 1495°C. Following firing, the as-fired thickness of Mo-Mn on all tensile buttons were inspected in three places using the x-ray fluorescence method. An average metallization thickness of 17.4 ± 1.9 μm was measured, with a minimum recorded thickness of 13.5 μm and a maximum thickness of 21.3 μm. Next, all tensile buttons were Ni-plated using a Watts bath solution carried out in a 7 gallon process tank. The current density was held constant at a value of 0.13 amps/in^2. Following the plating process, the buttons were wet hydrogen fired for 30 min. at 800°C. Following the sinter fire, parts were inspected for blisters. A number of fine blisters – ranging in size from 0.005 to 0.012 in. diameter, were observed on some of the tensile buttons, but these were judged as not detrimental to the intended use, and were allowed to proceed.

The tensile buttons were assembled for brazing in a brazing fixture which was intended to maintain alignment by means of a central rod and spacer assembly. Each tensile button pair included a 0.010 inch thick Kovar™ interlayer (OD=0.625 in., ID= .402 in.), along with 0.003 inch thick 50Au-50Cu alloy braze washers on either side of the Kovar interlayer. It should be noted that the fixture design used for this study did not fix the position of the the Kovar™ interlayer – i.e., it was allowed to "float" during brazing. Small amounts of Nicrobraze 520 braze cement were used to help center the braze preforms. Previous work with this braze cement has demonstrated that all of the residue burns off in a dry hydrogen atmosphere. A 304L stainless steel washer (weighing 20 gm.) was set on top of each of the button assemblies as an alignment weight.

Brazing was carried out in two identical batch furnace runs, with six pairs from each metallize sinter fire condition included in each run. The belljar-type furnace was equipped with four interior Molybdenum shelves, and was run with a dry hydrogen atmosphere at approximate –55°C dewpoint. For the present study, six button pairs were run on each of the two interior shelves of the furnace. The braze process had a nominal programmed peak temperature of 1007°C, as noted by the main heating element thermocouple. Three thermocouples, attached to the tensile button fixtures, were used to monitor the temperature closer to the work pieces. The maximum total time above liquidus (TAL) was 15 min. with a nominal ramp rate of 2°C per minute above the liquidus (1070°C), and a peak temperature range of 985-993°C.

RESULTS – SMALL TENSILE BUTTON STUDY

Twenty-four pairs of tensile buttons were fabricated and analyzed for hermeticity, strength, failure origin location, and joint microstructure. Hermeticity tests confirmed that all pairs of tensile buttons met helium leak rates equal to or less than 1×10^{-9} atm-cc/s. After tensile tests were completed, the fracture surfaces were examined using optical (OM) and Scanning Electron (SEM) microscopy to identify the failure origin location. Radial alignment of the Kovar™ interlayer with the alumina button half that remained together after tensile testing was measured with an Optical Gauging Products, Avant Model 250. Finally, longitudinal cross-sections, through the failure origin location, were made on representative samples to characterize the ceramic/metal joint microstructure.

Mechanical strength test data are presented in Table 1. The data were analyzed for the total population of tensile button samples, and broken into two groups, representing the two different metallization firing times. A histogram, Figure 1a, shows a normal strength distribution for the total population, as well as for the two firing times. Average tensile strength values are greater than 69.0 MPa (10 ksi) for the total tensile button and for both metallization firing-time groups. Statistical analysis of the data (see the values for standard deviation and Coefficient of Variance in Table 1) indicate that there is no significant strength difference between populations based on the two firing-time schedules. An average strength value of 69.0 MPa (10 ksi) is a conservative lower limit used to verify that the ceramic/metal joining process is robust. This lower acceptable strength limit is based on historical testing of Mo-Mn metallized 94% alumina ceramic joined to a Kovar™ interlayer using the 50Au-50Cu braze alloy. The data in Table 1 also show that the large standard deviations for the first three groupings shown allow the lower strength samples to dip below the 69.0MPa (10 ksi) minimum value. Examination of the tensile test data revealed a few samples with anomalously low strength values. These samples were examined optically and substantial misalignment of the Kovar™ interlayer/alumina button was correlated with the lowest failure strengths. All alumina button halves, with the Kovar™ interlayer attached, were inspected to quantify the misalignment of the Kovar™ interlayer and the alumina button. A plot of failure stress versus radial misalignment of the Kovar™ and the alumina, shown in Figure 1b, demonstrates the strong dependence of failure strength and interlayer misalignment. The trend curve shown in Figure 1b is based on a semi-log fit to the data as follows:

$$\text{Failure Stress (MPa)} = 108.18 * \exp[-34.882 * \text{Misalignment (in.)}]$$

A correlation coefficient (r^2) of 0.694 was obtained with this equation, which is understandably low in view of the significant scatter in the data. The strength data were further analyzed for test sample groups where the misalignment was less than 0.015, 0.010 and 0.005 inches. As samples with severe misalignment are removed from the population, the average strength is higher, and the standard deviation ranges become smaller. This observation resulted in the use of finite element analysis

(FEA) modeling of the tensile button geometry in order to quantify the effect of misalignment on stress development in the brazed tensile buttons.

Data Set	Sample Count	Failure Stress (MPa)	Std. Dev. (MPa)	Variance	Coeff. of Variance
Both Firings (all samples)	24	83.21	±23.59	556.5	28.35
Normal Firing	12	85.03	±15.87	252.0	18.67
Extended Firing	12	81.39	±30.07	904.4	36.95
Radial Misalign. <0.015 inch	21	89.26	±17.87	319.5	20.03
Radial Misalign. <0.010 inch	18	90.55	±15.34	235.3	16.94
Radial Misalign. <0.005 inch	7	93.80	±13.75	188.7	14.65

Table 1. Statistical summary of the tensile button tensile strength data.

Tensile button fracture surfaces and cross-sections through the joint were examined using OM and SEM. Micrographs of two samples, both processed with the extended Mo-Mn metallization firing time schedule, are shown in Figures 2 and 3. These samples represent high and low tensile strengths and demonstrate the relationship between Kovar™ interlayer misalignment and low strength. Figures 2a and 3a are optical images that show typical fracture surface morphology. The solid white arrows mark the fracture origins and dashed black lines show the direction of fracture propagation. Fratographic analyses of the separated tensile button surfaces show that the fracture always originates in the alumina near the Mo-Mn metallization layer, and propagates in the bulk alumina, in the metallization layer, and at the alumina/metallization interface to complete the fracture. Fracture origination in the alumina is expected because of low failure strength in ceramic materials compared to metals. Lack of failures at metal/metal interfaces indicates that good metallic bonding has occurred.

Optical micrographs, of cross-sections through the fracture origins, are shown in Figures 2b and 3b. White arrows mark the fracture origination location, and the dashed black boxes outline the joint interface regions that are shown at high magnification in Figures 2c and 3c. The micrographs in Figures 2b and 3b, respectively, show good and bad alignment of the Kovar™ interlayer between the two adjacent alumina members of the test sample. There is substantial extension of the Kovar™ interlayer beyond the alumina, Figure 3b, that correlates with the location of the fracture origination. In this test sample, there is also some misalignment of the alumina members. The fractographic analysis revealed a correlation between extreme Kovar™/alumina misalignment and fracture origination along the radial misalignment axis. Fracture origination in alumina in a uniform stress field is controlled by the location of the largest flaw, and flaws are typically randomly distributed. The correlation of alumina fracture origination, preferentially along a geometric axis, suggests that in some samples a non-uniform tensile stress was present in the joint that controlled the circumferential position of failure origination during mechanical testing.

A

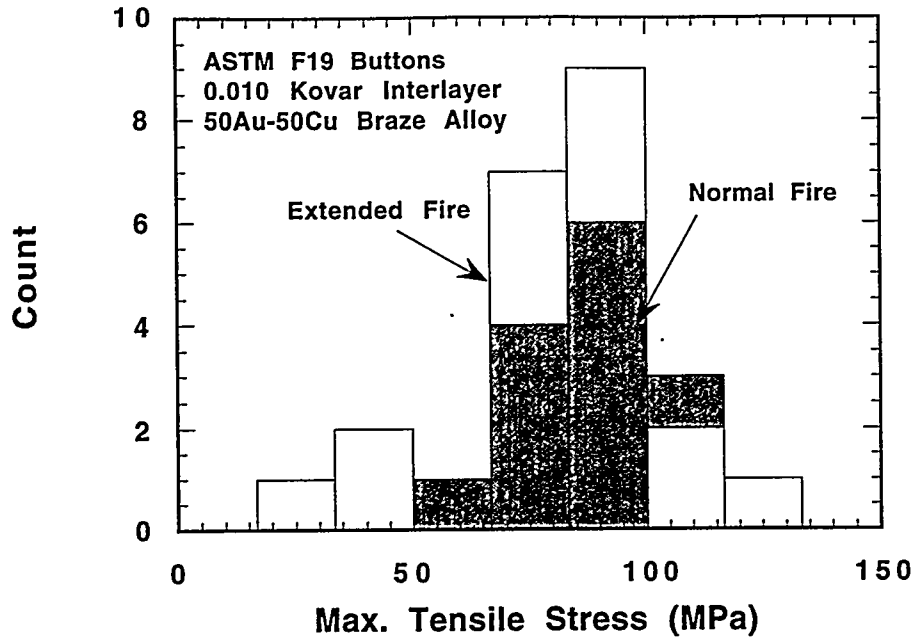

B

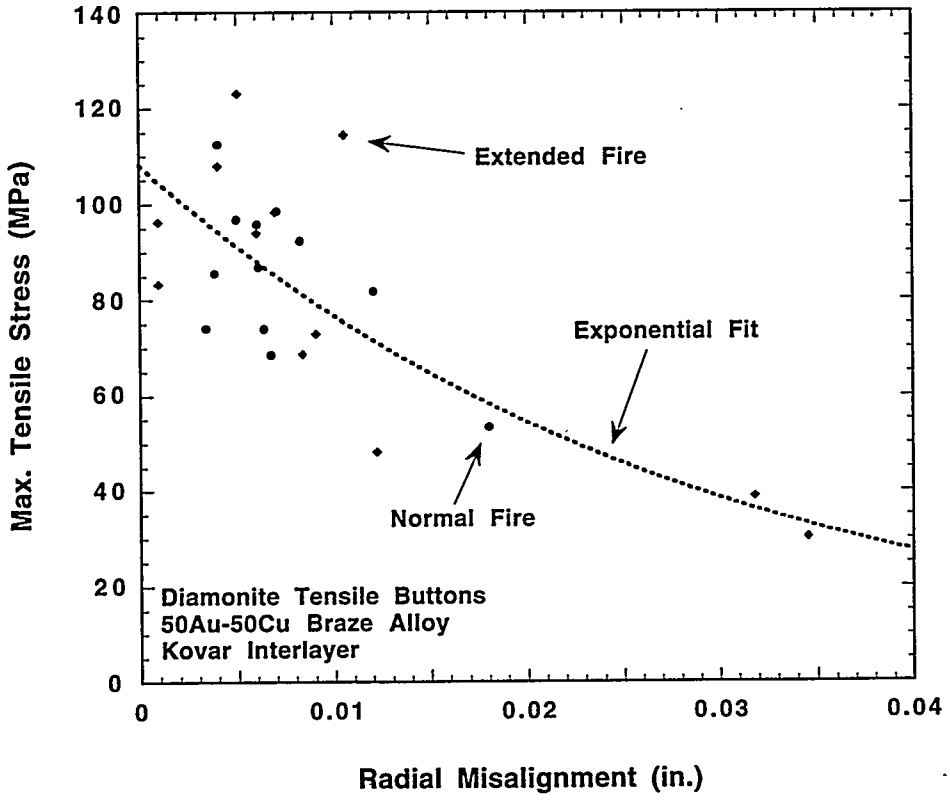

Figure 1. (a) Histogram showing the distribution of maximum strengths obtain with ASTM F19 tensile buttons for both normal and extended metallize sintering times. (b) Plot maximum strength as a function of Kovar™ interlayer misalignment. Note: 1 MPa is equal to 145.04 psi.

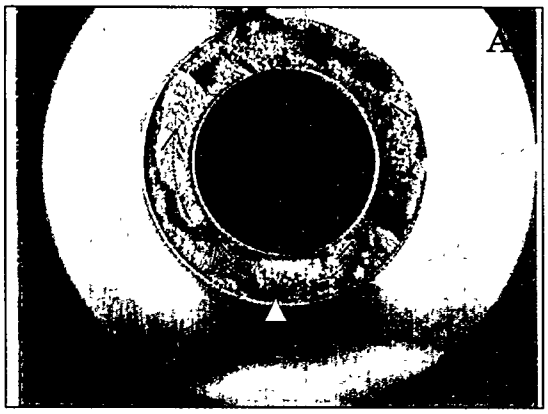

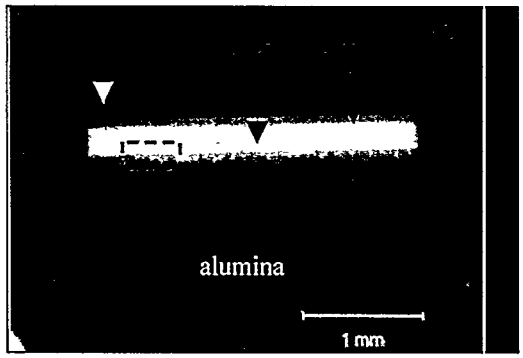

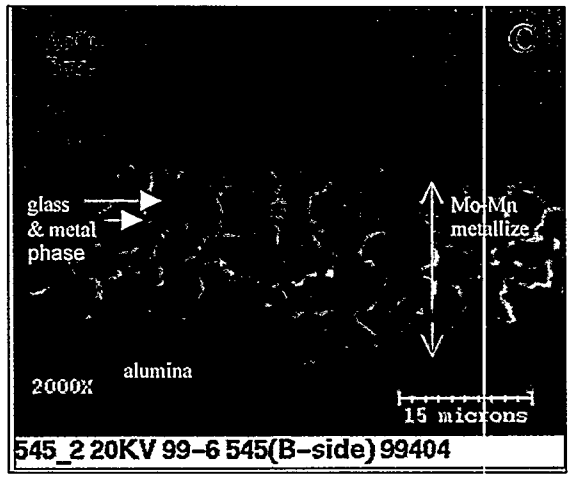

Figure 2. Photographs of sample #545 with a failure stress of 122.7 MPa (17.8 ksi), and a slight radial misalignment (0.00505 in.). (a) Low magnification view of fracture, indicating fracture origin and propagation. (b) OM micrograph, showing the fracture origin (white arrow). (c) SEM micrograph from the location shown in (b). Area fraction of the glass phase is 29.8%, metal 69.2%.

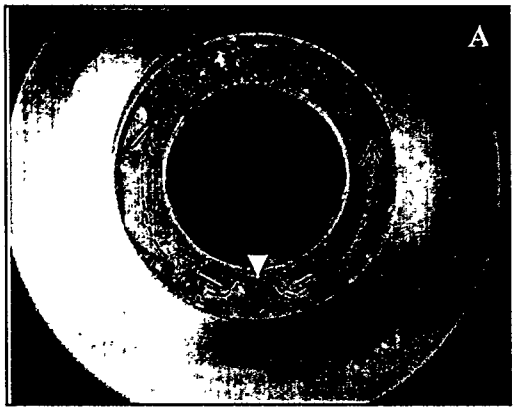

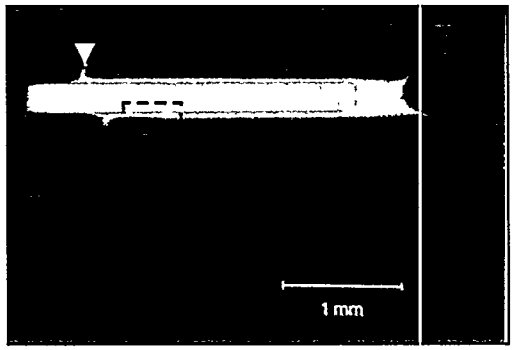

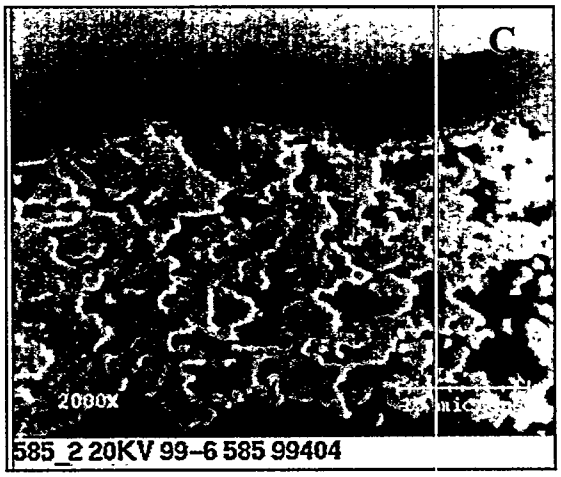

Figure 3. Photographs of sample #585 with a failure stress of 38.6 MPa (5.6 ksi), and significant radial misalign-ment (0.0318 in.). (a) Low magnification view of fracture, indicating fracture origin and propagation.(b) OM micrograph, including the fracture origin (white arrow). (c) SEM micrograph from the location shown in (b). Area fraction of the glass phase is 30.%, metal 70.%.

SEM examination of the cross-sectioned tensile buttons, comparing extended and normal firing times used to process the Mo-Mn metallization, revealed no significant differences in joint microstructure. The Mo-Mn metallization layer average thickness ranged from 18-28 μm. There is no relationship between thickness and firing time because thickness is controlled during the original screen printing process. However, glass phase development within the Mo-Mn metallization layer can be influenced by firing time. Micrographs in Figures 2c and 3c show there is good glass phase distribution in the metallization layer. Area fraction analysis of the glass and metal phases in four samples that represented normal and extended firing time of both thick and thin metallization layer conditions, resulted in very similar glass phase percentages, ranging from 28 to 30%. These cross-sections also show the remaining Ni-plating layer, nominally 5-10 μm, is a uniform thickness. The microstructural character of interfaces between the various members in the braze joint (ceramic, Mo-Mn metallization, Ni plate, Au-Cu braze alloy and Kovar™ interlayer) are indicative of a robust joint made using either the normal or extended metallization firing process.

In summary, there is no evidence that any part of the metallization or brazing process caused low failure strength observed in some of the samples tested in this study. Analysis of the mechanical test data and examination of fracture surfaces were used to identify the strong influence of interlayer misalignment on failure strength. That observation led to FEA modeling of the tensile button braze process and tensile testing to quantify residual stresses in the brazed assembly and stress development during the mechanical test. Results of those analyses are discussed in the next section.

EFFECT OF INTERLAYER MISALIGNMENT ON RESIDUAL STRESSES IN BRAZED TENSILE BUTTONS

In order to demonstrate the effect of interlayer misalignment on reduced failure stress in the F19 tensile button geometry, a series of finite element analysis (FEA) stress calculations were run. Two basic types of misalignment were studied: Case 1, where both tensile buttons are perfectly aligned, and the Kovar™ interlayer is subjected to varying amounts of radial misalignment; and Case 2, where the Kovar™ interlayer is perfectly aligned with the lower tensile button, and the top button is subjected to various amounts of axial misalignment. The 50Au-50Cu braze alloy was represented with viscoplastic (creep-plasticity) constitutive model (Refs. 8-9), while the Kovar™ was treated as a temperature dependent elastic-plastic material, and the alumina ceramic was represented as a perfectly elastic material. All calculations started at the braze solidification temperature with a stress-free condition, and calculated the effect of a linear, 1800 sec. furnace cooldown ramp to room temperature on residual stress development in the alumina ceramic. This was followed by axial loading to an applied load of 2500 lbs. Based on the ASTM F19 sample dimensions, this is equivalent to a nominal imposed stress of 13.90 ksi, or 95.8 MPa. In order to simplify the mesh geometry, the taper in the ceramic grip area in the ASTM F19 sample geometry was neglected.

The FEA stress calculations were run using the JAS3D FEA code (Ref. 10), run on a DEC Model 8400 computer equipped with 6 parallel processors. Due to the relatively complex geometry, 5×10^5 elements were used for each calculation, with a typical run time of 36 hrs. For Case 1 calculations, the regions on the ID of the sample where the Kovar interlayer was not present due to misalignment were assumed to be filled with braze alloy. For Case 2, the braze was meshed as uniformly solidified on top of each button, along with the fixed amount of radial displacement. The results of those calculations are shown below in Table 2. With respect to Case 1, the cylindrical angle θ has a value of 90° at the point of maximum outward displacement of the Kovar™ interlayer, while 270° is the point of maximum inward displacement of the Kovar™ interlayer. For Case 2, the maximum external offset of the top ceramic button and Kovar™ interlayer from the lower ceramic button is at θ =90°, while θ =270° represents the case of maximum internal offset, top to bottom.

Geometry	Axial Offset (in.)	Maximum Principal Stress in Ceramic at RT (MPa)	Location @RT	Max. Principal Stress @ RT + 2500 lbs. (MPa)	Location @RT + 2500 lbs.
Baseline	0.000	52.	Near OD (diam. =0.602)	117.	Near OD (diam. =0.607)
Case 1	0.012	319.	ID; $\theta \sim 15°$	346.	ID; $\theta \sim 30°$
Case 1	0.024	263.	NA	311.	NA
Case 1	0.036	210.	ID; $\theta = 90°$	273.	ID; $\theta = 90°$
Case 2	0.012	155.	ID; $\theta = 90°$	192.	OD; $\theta = 90°$
Case 2	0.024	142.	ID; $\theta = 90°$	263.	NA
Case 2	0.036	142.	ID; $\theta = 90°$	344.	NA

Table 2. Effect of either Kovar™ interlayer misalignment (Case 1) or Button-Button misalignment (Case 2) on maximum principal stress development in ASTM F19 brazed alumina ceramic tensile buttons. The applied load in the fourth column is equal to a nominal imposed stress of 13.90 ksi (= 95.8 MPa). Note: the OD of the tensile button sample is 0.625 inches.

Based on the FEA results shown in Table 2, the Case 1 interlayer misalignment is expected to cause higher stresses in the ceramic than for the Case 2 offset situation. The results for Case 1 geometry underscore the importance of minimizing the Kovar™ interlayer offset with the brazing fixture used for tensile button fabrication. Incidentally, based on the current braze fixture design for tensile buttons, the button to button offset (Case 2) is usually better controlled (to within 0.005 in.) than Kovar™ interlayer alignment. It is encouraging to note that the fracture origin indicated in Figure 2a is consistent with the maximum principal stress location for the "baseline" (no misalignment) geometry result shown in Table 2. However, most of the tensile buttons studied did show some button to button misalignment in addition to Kovar misalignment (e.g., see Figure 3b), and as such it is difficult to reconcile the fracture origin location predictions shown in Table 2 with experimental observations. These observations suggest the need for simulations that combine a linear combination of Case 1 and Case 2, in order to draw detailed comparisons with fractographic observations.

DISCUSSION

Two major lessons were learned from the STBS and subsequent FEA analysis: (a) the importance of good alignment (<0.005 inch offset) of the Kovar interlayer and (b) extended firing of the metallize layer is permissible. To remedy the Kovar interlayer misalignment problem, two steps were taken: (a) the Kovar™ interlayer was given a slightly larger footprint (ID decreased to 0.392±0.003 in, OD increased to 0.635±0.003) and (b) the outside diameter of the alumina ceramic alignment sleeve – which controls the ID alignment of the Kovar™ interlayer – was increased to 0.388±0.001 in. It is anticipated that these two modifications will improve the consistency of the tensile button alignment. A related lesson is that the relatively small blisters encountered with the Ni plating do not appear to affect hermeticity. We suppose that Ni plate blisters would have to be substantially larger to cause hermeticity problems.

We have also begun fabrication of parts for the LTBS. As indicated above, the LTBS is a follow-on to the Small Tensile Button Study, and incorporates the lessons learned from the earlier study. The LTBS will be split between two different ceramics: (a) the Diamonite P-3142-1 ceramic and (b) SANDI-94 ceramic. The latter is a 94% ceramic which is intended to duplicate the 94ND2 grade ceramic which has been described previously (11). Besides the ceramic type, the following process variable parameters will be examined using low/medium and high settings: (a) TAL, (b) Peak braze temperature, (c) Ni plate thickness, (d) Braze washer thickness, and (e) Metallize thickness. We hope to present results from the LTBS at the symposium associated with this proceedings volume.

CONCLUSIONS

The results of the Small Tensile Button Study have demonstrated that control of Kovar™ interlayer misalignment is important in order to fully understand the distribution of failure stresses in brazed ASTM F-19 tensile buttons. In addition, the metallization sinter fire time has an apparent acceptable range between 45 and 120 minutes at 1495°C, and small Ni plate blisters do not affect hermeticity results. Modifications to the tensile button brazing fixture will be implemented for use in the Large Tensile Button Study.

Fractographic observations of well-aligned tensile button pairs indicated that fracture originates near the OD of the tensile button braze joint, within the alumina ceramic. These results are consistent with the FEA computed location of maximum principal stress in the ceramic. Two types of misalignment were studied using FEA stress analysis, and these results suggest that Kovar interlayer misalignment leads to higher stresses than top/bottom button misalignment. Detailed fractographic comparisons with FEA results were not possible due to the "mixed mode" nature of the interlayer and top/bottom button misalignment.

ACKNOWLEDGMENTS

We would like to acknowledge the participation of the following SNL personnel in these studies: Steve Crowder, for guidance in the statistical design of experiments, Matt Senkow for furnace brazing, Paul Morrison for metallization, and George Edgerly for Ni plating. We would also like to acknowledge the peer review of this manuscript by F. M. Hosking, along with his help in making the Small Tensile Button Study a success.

Kovar™ is a registered trademark of Carpenter Technology Corporation.

REFERENCES

1. Kohl, W. H.., 1967. Handbook of Materials and Techniques for Vacuum Devices:446-449. New York, NY: Reinhold Publishing Corporation.
2. Bertolotti, R. L., 1974. Thermal expansions of Kovar and Ceramvar and seals of these materials to alumina. Report No. SAND74-8003, September, Sandia Laboratories.
3. Stephens, J.J.; Burchett, S. N.; and Hosking, F. M. 1991. Residual stresses in metal-ceramic brazes: effect of creep on finite element analysis results. Metal-Ceramic Joining. Eds. P. Kumar and V. A. Greenhut: 23-41. Warrendale PA: TMS.

4. Stephens, J.J.; Burchett, S. N.; and Jones, W. B. 1992. Stress relaxation of brazements. Advances in Electronic Packaging, 1992. Eds. W. T. Chen and H. Abe: 362-372. New York, NY: ASME.

5. Stephens, J.J and Hlava, P. F. 1994. Reducing the inadvertent alloying of metal/ceramic brazes. Low Thermal Expansion Alloys and Composites Eds. J. J. Stephens and D. R. Frear: 59-77. Warrendale, PA: TMS.

6. Hosking, F. M.; Gianoulakis, S. E.; and Malizia, L. A. 2000. Thermal and fluid flow brazing simulations. (in this volume)

7. ASTM.F19-64. Standard test method for tension and vacuum testing metallized deramic seals. 1996 Annual Book of ASTM Standards, Volume 10.04 (Electronics (I)): 25-28. West Conshohocken, PA: American Society for Testing and Materials.

8. Neilsen, M. K.; Burchett, S. N.; Stone, C. M. and J. J. Stephens, J. J. 1996. A viscoplastic theory for braze alloys. Report No. SAND96-0984, April, Sandia National Laboratories.

9. Stephens, J. J. 1999. Tensile creep properties of the 50Au-50Cu braze alloy. Advanced Materials for the 21st Century: The Julia R. Weertman Symposium. Eds. Y-W. Chung, D. C. Dunand, P. K. Liaw and G. B. Olson: 117-128. Warrendale, PA: TMS.

10. Blanford, M. L. 1999. JAS3D – a multi-strategy iterative code for solid mechanics analysis, Users's Instructions, Release 1.6. Internal memo. Sandia National Laboratories.

11. Hellmann, J. R. 1986. Alumina processing and properties characterization workshop, February 3, 1986. Report No. SAND86-1224: 110-118, August. Sandia National Laboratories.